Determination of the Chelating Site Preferentially Involved in the Complex of Lead(II) with Caffeic Acid: A Spectroscopic and Structural Study

L. Boilet, J. P. Cornard,* and C. Lapouge

Laboratoire de Spectrochimie Infrarouge et Raman (UMR 8516 - Université de Lille I - CNRS), Bât. C5, Université des Sciences et Technologies de Lille, 59655 Villeneuve d'Ascq Cedex, France

Received: May 27, 2004; In Final Form: December 8, 2004

The complexation of lead(II) with mono-deprotonated caffeic acid in aqueous solution (pH = 6.50) has been investigated by UV−visible, fluorescence, and vibrational spectroscopies combined with quantum chemical calculations (DFT). The caffeate ion presents two chelating sites in competition: the carboxylate and the catechol functions. Electronic spectroscopies highlighted two different complexed forms with, respectively, 1:1 and 2:1 stoichiometry. The 1:1 complex predominates for low lead concentrations, even if the second complexed form appears before the first chelating site is fully occupied. Both spectroscopic data and calculations reveal that Pb(II) preferentially coordinates with the carboxylate function, in opposition with previous results found for the Al(III) complexation, where the catechol group presents the greater complexing power. The structural and vibrational modifications between the mono-deprotonated ligand and 1:1 complex engendered by the chelation are discussed. Water molecules have been added on the Pb ion to modify its coordination, and structures of $Pb(H_2CA)(H_2O)_n^+$ with $n = 0-4$ were optimized. Calculations of theoretical frequencies have permitted us to propose a tentative assignment of infrared and Raman spectra of complexed species.

1. Introduction

Humic acids (HA) are macromolecular compounds with a very complex and heterogeneous structure. The size, chemical composition, structure, and functional groups of HA may change significantly with the origin and the age.[1] Moreover, due to the large number of complexing sites involving different functional groups (carboxylic, phenolic, salicylic, amine ...)[2] and different affinities for heavy metal cations, little is known about the complexation properties of humic acids and notably the structure of metal-binding sites. To obtain further information about the complexation mechanism of lead(II) ion in aqueous solutions, we propose to study the complexation processes with a simple model molecule: caffeic acid (3,4-dihydroxy-*trans*-cinnamic acid), which is known to constitute a precursor compound in the formation of soil organic matter and to participate in the transport of ionic metals present in the soil.[3] Caffeic acid (H_3-CA) possesses two possible chelating sites in competition: the catechol (*ortho*-dihydroxybenzene) and the carboxylic acid functions (see Figure 1). These two functions are the major ligands of humic substances able to coordinate metal ions. All spectroscopic measurements were recorded at pH = 6.50. Indeed, at this pH value (close to the soils' pH), the carboxylic acid function of caffeic acid is totally deprotonated (pK_a (COOH) ∼ 4.45)[4,5] and only the mono-deprotonated species is present in solution. In the following, caffeate will be noted (H_2CA^-). The main objectives of this study are first to determine the stoichiometric composition and the formation mechanism of the different complexes obtained between caffeic acid and Pb(II) by both UV−visible and fluorescence measurements. From this mechanism, a hypothesis on the first complexing site of caffeic acid will be proposed. In a second step, vibrational spectroscopies (FT-Raman and infrared) combined with quantum chemical calculations are used to confirm the site preferentially implicated in the complex formation and to study the structural modifications of the ligand engendered by the chelation for low Pb(II) concentration.

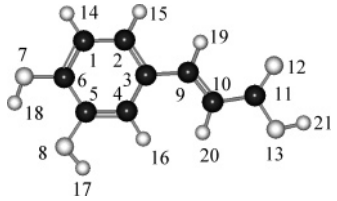

Figure 1. Representation and atomic numbering adopted for caffeic acid molecule H_3CA.

2. Experimental Section

2.1. Reagents and Preparative Methods. Caffeic acid was obtained from Aldrich. Water was deionized. Lead nitrate and sodium chloride were used without purification. The pH of all solutions was maintained at pH 6.50 and adjusted using HCl and NaOH as required. In all cases, spectra have been corrected from dilution. The ionic strength has been adjusted to 0.1 by sodium chloride. Caffeic acid concentration was 5×10^{-5} M and 2×10^{-5} M for the UV−visible and fluorescence measurements, respectively. The complex stoichiometry was determined by the molar ratio method.[6] Infrared and Raman measurements where achieved from the solid complex. A yellow precipitate was obtained by addition of 1 cm^3 of 5×10^{-3} M $Pb(NO_3)_2$ to 10 cm^3 of 5×10^{-3} M solution of caffeic acid. The pH factor was kept at 6.5 by addition of NaOH solution. The precipitate was filtered and dried under vacuum and in the dark to avoid photooxydation.

2.2. Instrumentation. To minimize the degradation of the samples, solutions for the absorption and fluorescence measurements were circulating in a flow cell with 1-cm path length.

* Corresponding author. Tel.: + 33-3.20.43.69.26. Fax: + 33-3.20.43.67.55. E-mail: cornard@univ-lille1.fr.

10.1021/jp047703d CCC: $30.25
Published on Web 02/12/2005

UV−visible spectra were run at room temperature on a double-beam spectrophotometer (Cary 100-Varian). Fluorescence spectra were recorded using a Fluoromax-3 (Jobin-Yvon) spectrofluorimeter with slit width of 5 nm. Three-dimensional spectra were acquired by incrementing the excitation wavelengths from 260 to 450 nm, in 2-nm steps, while scanning emission from 300 to 350 nm. In the final excitation−emission matrix (EEM) plots, the excitation wavelengths are plotted on the *y*-axis and the emission wavelengths are plotted on the *x*-axis. The third dimension represents the relative intensity.

The Fourier transform (FT) Raman spectra were recorded with 4 cm^{-1} resolution on a Bruker IFS 88 W instrument equipped with an FRA 106 FT-Raman accessory. The excitation in the near-infrared range (1.06 μm) permits one to avoid fluorescence emission of studied samples. FT-IR spectra were recorded with a Bruker Vector 22 spectrometer operating with a resolution of 2 cm^{-1}. A concentration of approximately 2% in potassium bromide has been used for the complex 1:1.

2.3. Calculations. The DFT calculations have been performed with the GAUSSIAN 03 quantum chemical package[7] implemented on a IBM SP/Power 4 machine located at IDRIS (CNRS - France). Geometry optimizations and harmonic vibrational frequency calculations of caffeate and of its complexes with Pb(II) were obtained by using the three-parameter hybrid functional B3LYP.[8,9] We adopted the Los Alamos effective core potential double-ξ (LanL2Dz) basis set for Pb and the 6-31G-(d,p) one for the other atoms (including polarization functions, to correctly take into account the intramolecular H-bonding in free ligand). For the complex, water molecules have been added to the lead atom to simulate different environments of this ion. Computed vibrational frequencies were scaled by a factor 0.972 for both free ligand and complexes. This value corresponds to the average of ratios experimental/calculated frequencies for each compound. Indeed, as scaling factors depend on the level of theory, the basis set, and the studied molecules,[10] we preferred to determine the best factor of our system, instead of using a predefined one. It is important to note that the same scaling factor has been used in a previous vibrational analysis of caffeic acid and of its complex with Al(III).[11]

The formation constants of the complexes of H_2CA^- were estimated by using a multivariate data analysis program for modeling and fitting equilibrium titration 3D data sets obtained from experimental measurements. The fluorescence spectra were refined using the SPECFIT software (version 3.0.32).[12] The set of spectra obtained at variable lead(II) concentration were treated by evolving factor analysis (EFA)[13] in order to determine the number of different species in the system and the pure fluorescent spectrum of each complex. The SPECFIT software has also been used to estimate the stability constants (β) of the complexes and the standard deviation (σ) of each value.

3. Results and Discussion

3.1. Stoichiometry and Formation Constants of the Complexes. Absorption spectra of caffeic acid at pH = 6.50 in aqueous solution (5×10^{-5} M) with different concentrations of $PbNO_3$ are presented in Figure 2. The first spectrum obtained in the absence of lead(II) is characteristic of the mono-deprotonated caffeic acid and presents two bands located at 286 and 312 nm.[14] Through the addition of Pb(II), these two bands decrease in intensity, while a band around 350 nm slowly increases with the amount of lead added. For molar ratios lower than 0.3, an isosbestic point is observed at 325 nm, indicating the presence of two species in equilibrium and therefore the formation of a first complex. For ratios greater than 0.3, the caffeate absorption bands still decrease, concomitantly with the increase of the band around 350 nm, but the absence of a real isosbestic point reveals that at least three different absorbing species are present simultaneously in solution: the formation of a second complexed form begins before all the caffeate ions are already engaged in a first complex. $[PbNO_3]/[H_2CA^-]$ ratios greater than 3 were impossible to obtain due to the precipitation of the lead(II) hydroxide. By comparison with the data previously obtained for the complexation of aluminum(III) by caffeic acid,[15] it can be deduced that the efficiency of complexation of lead is lower than this observed for aluminum where important spectral evolution is observed for a small amount of added metal. Other measurements carried out in water at pH = 5 or in pure methanol, where the carboxylic acid function is protonated, do not lead to complexation of Pb(II), as previously observed.[5] This first result may suggest that chelation occurs only when the carboxylic acid group is deprotonated.

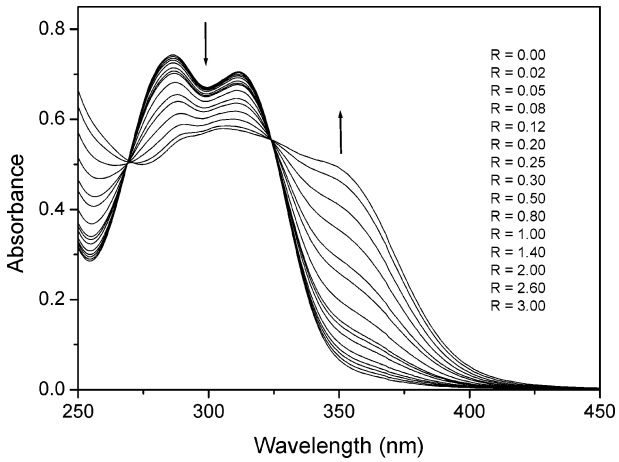

Figure 2. Absorption spectra of caffeic acid (5×10^{-5} M) in aqueous solution (pH = 6.50) in the absence and presence of Pb(II). The molar ratios $R = [PbNO_3]/[H_2CA^-]$ are indicated on the right of the figure.

The molar ratios method was used to determine the stoichiometry of the complexes of H_2CA^- with lead(II). In this method, ideally two straight lines are obtained when the absorbance at one wavelength is plotted versus the metal-to-ligand ratio. The intersection point of these two lines corresponds to the stoichiometric ratio upon interpolation to the molar ratio axis. The molar ratios plots at 285 and 350 nm show inflection at $R = [PbNO_3]/[H_2CA^-] = 1$ and 2, respectively, indicating the formation of two different complexes with stoichiometry Pb(II)/H_2CA^- of 1:1 and 2:1, respectively. For this latter, one can suppose that the two chelating sites of the ligand are engaged in the complex formation. Due to the weak spectral evolutions engendered by the complexation, pure absorption spectra of the different complexes, necessary to calculate the stability constants, were impossible to obtain precisely.

In Figure 3 are presented the emission fluorescence spectra of the mono-deprotonated caffeic acid in aqueous solutions (2×10^{-5} M) obtained with excitation at 330 nm (A) and 350 nm (B) for several $[Pb^{2+}]/[H_2CA^-]$ molar ratios between 0 and 9. For all measurements, pH was maintained constant at 6.5. In Figure 3A, the first spectrum obtained without lead is characteristic of the mono-deprotonated form of caffeic acid. With the addition of small amounts of Pb(II), the band slowly decreases and an isosbestic point appears around 438 nm. For molar ratios higher than ~0.3, this isosbestic point disappears, suggesting the presence of at least three different species as observed by UV−visible spectroscopy. Then a new band is clearly growing with the amount of lead with a maximum around

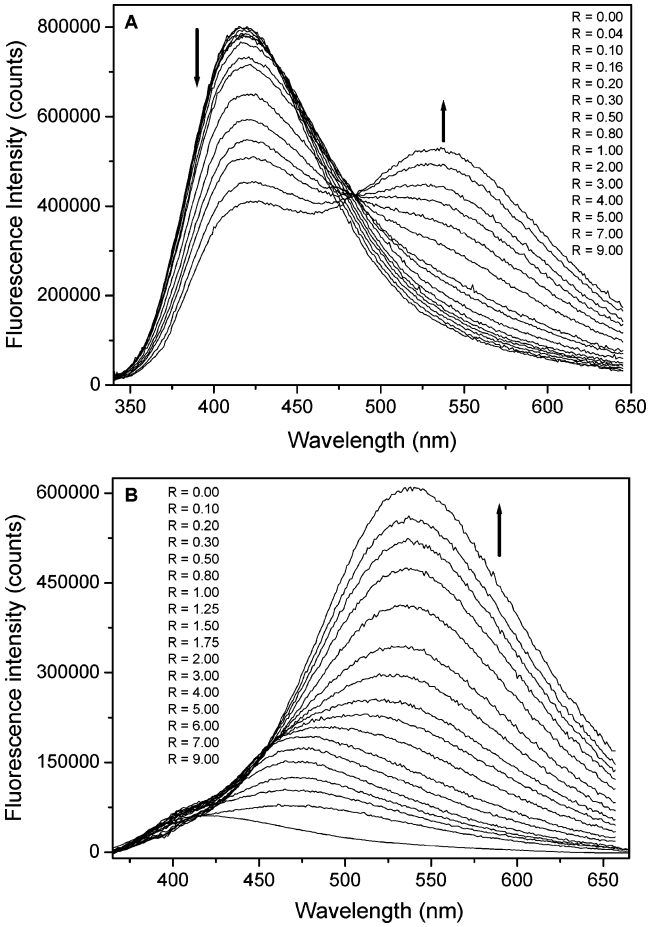

Figure 3. Emission fluorescence spectra of caffeic acid H_2CA^- (2×10^{-5} M) in aqueous solution (pH = 6.50) in the absence and presence of Pb(II) with excitation at 330 nm (A) and 350 nm (B). The molar ratios $[PbNO_3]/[H_2CA^-]$ are indicated on the figure. The background spectrum ([NaCl] = 0.1 M) has been subtracted.

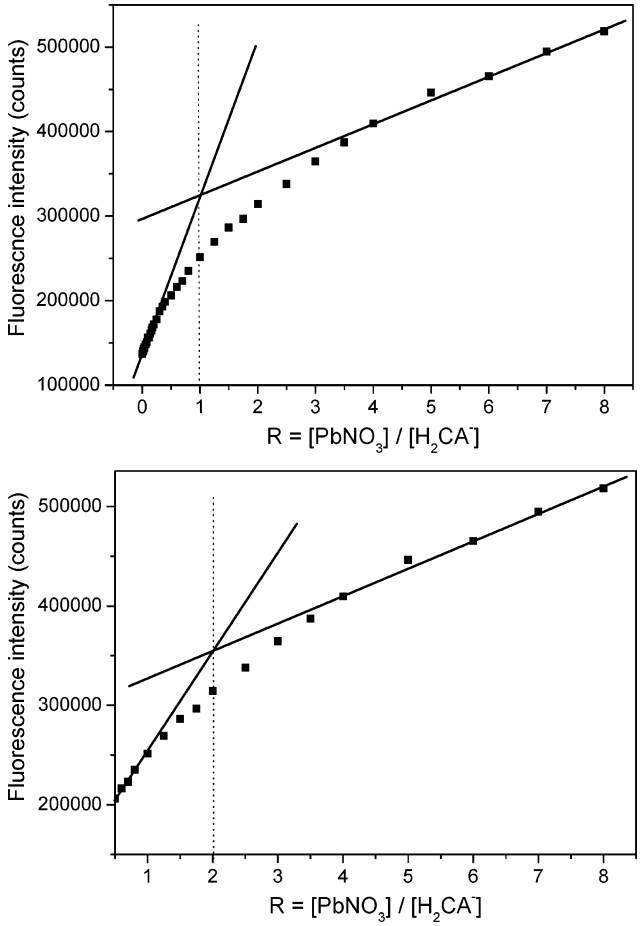

Figure 4. Fluorescence intensity (λ_{exc} = 330 nm) versus $[PbNO_3]/[H_2CA^-]$ molar ratios plots at λ_{em} = 540 nm with two different abscissa scales.

540 nm, whereas the initial caffeic acid band ($\lambda_{em,max}$ = 418 nm) seems to be still present.

In Figure 3B are shown the fluorescence spectra obtained after photoexcitation at 350 nm. This wavelength, located in the bottom of the absorption band of H_2CA^-, was chosen to minimize the contribution of the mono-deprotonated caffeic acid in the fluorescence spectrum. The initial spectrum ($\lambda_{em,\ max}$ = 418 nm) is characteristic of caffeate, with the same shape as this observed in the first spectrum in Figure 3A. With addition of lead, a first fluorescence band that could be assigned to the first complex clearly grows ($\lambda_{em,\ max}$ = 475 nm). For greater molar ratios, a new band ($\lambda_{em,\ max}$ = 540 nm) appears; this band intensity has not yet reached a maximum for a ratio of 9, suggesting that the complexation process is not completed. The molar ratios method applied to the fluorescence spectra set validates the results obtained with the UV−visible absorption spectra, since 1:1 and 2:1 stoichiometries are found. Indeed, the molar ratio plot at 540 nm shows inflections at ratios 1 and 2 (Figure 4).

From the fluorescence spectra obtained with an excitation at 350 nm, the determination of the number of different species was estimated by the EFA method with the SPECFIT software. Three distinct components were found corresponding to the free caffeic acid (H_2CA^-) and the two complexes with 1:1 and 2:1 stoichiometry, provisionally noted PbL and Pb_2L, respectively. The fluorescence spectra of pure species are presented in Figure 5. To estimate the stability constants, a numerical treatment of the fluorescence spectra has been carried out with a model implicating two complexes with 1:1 and 2:1 stoichiometry. The model best-fitting the experimental data gives the following stability constants: $\log \beta = 5.77 \pm 0.47$ and $\log \beta = 10.80 \pm 0.46$ for the 1:1 and 2:1 complexed forms, respectively. This result comes from the following reaction between lead and ligand (L):

$$a\mathrm{Pb} + b\mathrm{L} \leftrightarrow \mathrm{Pb}_a\mathrm{L}_b$$

with the corresponding stability constant:

$$\beta = \frac{[\mathrm{Pb}_a\mathrm{L}_b]}{[\mathrm{Pb}]^a[\mathrm{L}]^b}$$

The concentration variations of the different species versus the quantity of lead added is illustrated in Figure 6A. These curves confirm that the complexation of the second site (formation of the Pb_2L complex) largely starts before the complexation of the first site is completed. One can estimate that Pb(II) begins to coordinate to the second chelating site from a ratio ~0.3 (Figure 6B). Moreover, as observed previously, for the largest molar ratio used in this study (R = 9.0), a large amount of caffeate ions (between 15 and 20%) remains noncomplexed.

Very close stability constants and distribution curves were obtained when the same model was used to fit the fluorescence data obtained with excitation at 330 nm.

3.2. Determination of the First Site Implicated in the Complexation. The aluminum complexation with caffeic acid has been previously studied by potentiometric titrations (in water),[16,17] UV−visible measurements (in water for different

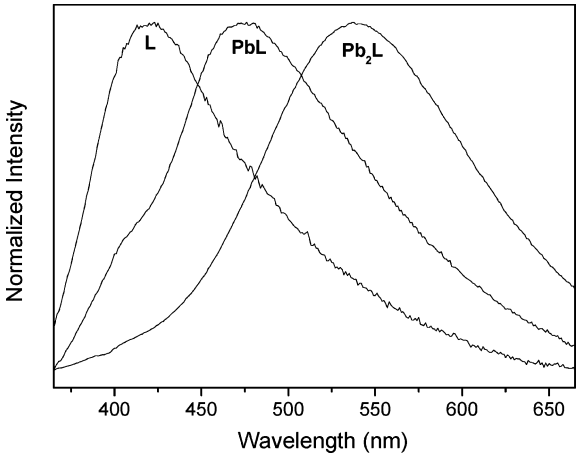

Figure 5. Normalized fluorescence spectra of mono-deprotonated caffeic acid (L), 1:1 (PbL) and 2:1 (Pb_2L) complexes determined by the SPECFIT software.

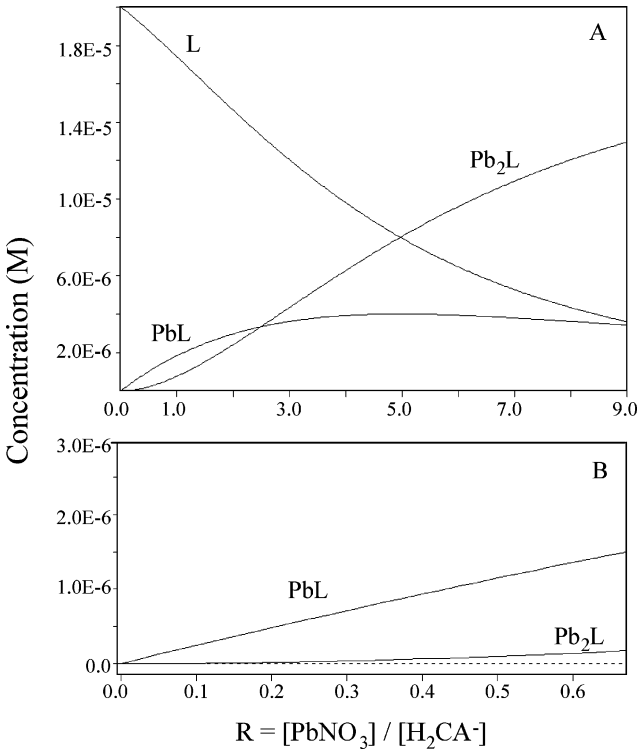

Figure 6. Distribution curves of lead complexes with caffeic acid in water (pH = 6.50) as a function of $[PbNO_3]/[H_2CA^-]$ molar ratios. (A) For ratios between 0 and 9. (B) For ratios between 0 and 0.7.

pH values and in methanol),[11,15] and quantum DFT calculations.[11] In all cases, it has been shown that the first complexing site is the catecholate moiety and that formation of the 1:1 complex begins to occur from pH = 3.[16] In this study, we observed that no complexation of lead(II) occurs when the carboxylic acid function is protonated, i.e., in pure methanol or in water for pH ≤ 5.0. These first results suggest that Pb(II) presents a comportment very different from that of Al(III) and would be first complexed on the carboxylate group.

In Figure 7 are presented three fluorescence excitation−emission matrix plots (EEM) obtained for different lead(II)/caffeate molar ratios. In the absence of lead (Figure 7A), three distinct peaks can be observed. The two peaks ($\lambda_{em} \sim 420$ nm, $\lambda_{exc} \sim 285$ nm) and ($\lambda_{em} \sim 420$ nm, $\lambda_{exc} \sim 310$ nm) can easily be ascribed to the free mono-deprotonated caffeic acid (see the first spectrum in Figures 2 and 3A). On the contrary, the third

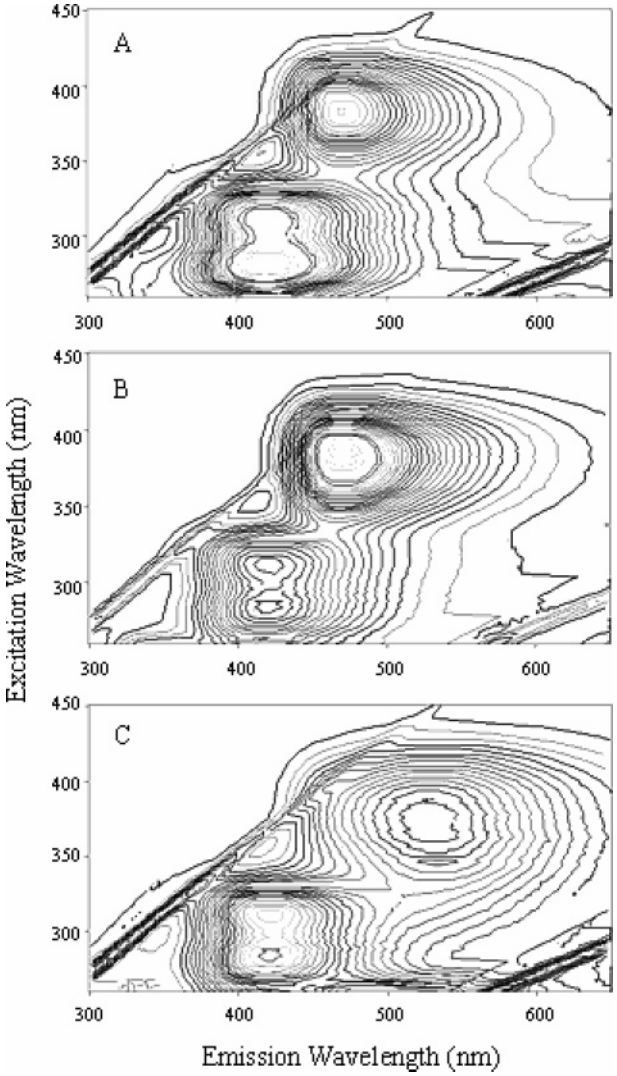

Figure 7. Fluorescence excitation−emission matrix plots of caffeic acid in 0.1 M NaCl (pH = 6.50) for different $[Pb(II)]/[H_2CA^-]$ ratios: (A) $R = 0.0$; (B) $R = 0.3$; (C) $R = 4.0$.

peak ($\lambda_{em} \sim 470$ nm, $\lambda_{exc} \sim 380$ nm) cannot be attributed to caffeate, since no absorption is observed at 380 nm in Figure 2. In the literature, many authors have shown that catechol groups can undergo oxidation to orthoquinones, which are unstable and can easily react to give products that absorb at longer wavelengths.[14,18−20] This third peak has already been observed on an EEM recorded at pH = 9.5 and was ascribed to the ionized phenolates ions of caffeic acid.[20] However, it is known that, at this pH value, unstable quinone intermediates are easily formed. So we rather propose to ascribe this peak to an oxidation product of caffeic acid. This hypothesis is reasonable insofaras the obtaining of an EEM necessitates ∼10 h of recording, and during this time, the sample is continuously irradiated by the excitation beam. A photodegradation is consequently observed. This degradation is greatly reduced and becomes negligible in the recording of spectra of Figure 3, due to a shorter irradiation time. However, even recording a single spectrum requires a flow of the solution to avoid photodegradation. Figure 7B represents the EEM recorded for a $[Pb(II)]/[H_2CA^-]$ molar ratio of 0.3. For this ratio, only the 1:1 complex is expected to be observed and around 95% of caffeate is supposed to be free (see Figure 6B). The three same peaks are observed: the two peaks corresponding to the mono-deprotonated free ligand and the third peak ascribed to the oxidation

TABLE 1: Calculated Bond Lengths (Å) of the Deprotonated Caffeic Acid (H_2CA^-) and of Its 1:1 Complex $Pb(H_2CA)(H_2O)_n^+$ ($n = 0-4$)[a]

	H_2CA^-	$Pb(H_2CA)^+$	$Pb(H_2CA)(H_2O)^+$	$Pb(H_2CA)(H_2O)_2^+$	$Pb(H_2CA)(H_2O)_3^+$	$Pb(H_2CA)(H_2O)_4^+$
C_1C_2	1.396	1.383	1.387	1.388	1.389	1.389
C_2C_3	1.408	1.418	1.413	1.411	1.410	1.410
C_3C_4	1.412	1.423	1.420	1.419	1.418	1.418
C_4C_5	1.385	1.376	1.378	1.379	1.380	1.380
C_5C_6	1.404	1.426	1.422	1.420	1.419	1.419
C_6C_1	1.391	1.400	1.397	1.396	1.395	1.395
C_3C_9	1.466	1.426	1.434	1.439	1.441	1.443
C_9C_{10}	1.343	1.377	1.369	1.364	1.362	1.361
$C_{10}C_{11}$	1.543	1.413	1.425	1.436	1.442	1.446
C_6O_7	1.375	1.334	1.340	1.342	1.344	1.344
C_5O_8	1.388	1.362	1.365	1.367	1.368	1.368
$C_{11}O_{12}$	1.257	1.315	1.305	1.301	1.286	1.294
$C_{11}O_{13}$	1.259	1.312	1.309	1.300	1.305	1.292
C_1H_{14}	1.086	1.084	1.084	1.084	1.084	1.084
C_2H_{15}	1.086	1.086	1.086	1.086	1.086	1.086
C_4H_{16}	1.088	1.086	1.086	1.087	1.087	1.087
O_8H_{17}	0.965	0.966	0.966	0.966	0.965	0.965
O_7H_{18}	0.969	0.972	0.972	0.971	0.971	0.971
C_9H_{19}	1.090	1.088	1.089	1.089	1.089	1.089
$C_{10}H_{20}$	1.092	1.083	1.084	1.084	1.084	1.084
$O_{12}Pb$		2.153	2.186	2.223	2.292	2.252
$O_{13}Pb$		2.150	2.191	2.221	2.263	2.381
PbO_{22}			2.367	2.484	2.554	2.566
PbO_{23}				2.484	2.451	2.419
PbO_{24}					2.575	2.512
PbO_{25}						3.499

[a] Atoms 22−25 are the oxygen atoms of water molecules.

product. However, the relative intensities of the two first-mentioned peaks have significantly changed; although the most intense peaks were the caffeate peak in the absence of lead, the oxidation product's peak becomes preponderant with the addition of only a small amount of Pb(II). This result suggests that the oxidation process is more efficient with the addition of lead, implying that the first complex of caffeic acid can be oxidized too, and consequently that the catechol function is not complexed. As a confirmation, for a molar ratio of 4.0 (see Figure 7C), a new peak appears ($\lambda_{em} \sim 530$ nm, $\lambda_{exc} \sim 370$ nm) that we ascribe mainly to the 2:1 complex that is dominant for this ratio. The oxidation peak is no longer observed, the catecholate moiety being largely complexed by lead that prevents the oxidation process.

All these spectroscopic data suggest that lead is first complexed with the carboxylate function of caffeic acid. To confirm this assumption, quantum chemical calculations have been undergone. First, energies of $Pb(H_2CA)^+$ with Pb on the carboxylate site and $Pb(CA)^-$ with Pb on catecholate site have been minimized and corrected for zero-point vibrational energy (ZPVE). To make a comparison, the ZPVE-corrected energies of two water molecules on one hand and two H_3O^+ on the other hand have been added to the energies of $Pb(H_2CA)^+$ and $Pb(CA)^-$, respectively, to maintain a constant number of atoms in both cases. The so-determined energies are $E = -804.008348$ and -803.636376 Hartrees for $Pb(H_2CA)^+$ and $Pb(CA)^-$, respectively, suggesting that the first envisaged complex is more stable by about 233 kcal mol^{-1} than the other one. This confirms that the carboxylate group is the first site involved in the complexation mechanism, as deduced from spectroscopic data.

3.3. Structural Analysis of the First Complex between Lead(II) and Caffeate. In the continuation of this article, we will focus our attention on the 1:1 complex, involving the carboxylate group, which is predominant for a low amount of lead(II) added. DFT calculations have been carried out on the caffeate and $Pb(H_2CA)^+$ complex in order to determine the structural modifications of the ligand engendered by chelation. As the complex formation occurs in aqueous solution, it appears interesting to study the influence of water molecules on the complex structure, knowing that the coordination of Pb(II) is frequently challenging to define.[21−23] Geometrical parameters of deprotonated caffeic acid H_2CA^- and $Pb(H_2CA)(H_2O)_n^+$ ($n = 0-4$) complexes are reported in Tables1 and 2. Dihedral angles of caffeate are not specified because they remain planar in all complexes. Whatever the starting geometry of the species (monodentate or bidentate), calculations converge to a bidentate complex. The caffeate benzene ring shows a low pseudo-quinoidal form, mainly due to the presence of an intramolecular hydrogen bond (O_8---H_{18}).[11] Comparison of bond lengths in H_2CA^- and $Pb(H_2CA)^+$ ($n = 0$) exhibits a strong effect on the electronic distribution due to coordination of Pb(II). The ring enforced its quinoidal character with a decrease of the C_1C_2 and C_4C_5 bond lengths and an increase of all the others. Consequently, the C_6O_7 bond length is considerably reduced (0.04 Å) with respect to its value in caffeate, whereas the C_5O_8 bond length is less affected. These effects are accompanied by a much more pronounced delocalization along the chain, with an increase of the central C_9C_{10} bond length and a decrease of the two adjacent ones C_3C_9 and $C_{10}C_{11}$. The ring bond angles evolve to a more symmetric moiety, by getting closer to 120°. The carboxylate entity is strongly modified with an increase of approximately 0.06 Å for the $C_{11}O_{12}$ and $C_{11}O_{13}$ bond lengths and a tightening of 16° of the $O_{12}C_{11}O_{13}$ angle. The coordination of Pb(II) symmetrically occurs on the COO^- group.

The Pb^{2+} ion can coordinate a variable number of ligands, giving rise to two coordination types: holodirected and hemidirected (the ligands are not distributed through the entire sphere surrounding the lead atom). The hemidirected distribution is due to the presence of the 6s electron lone pair on the Pb atom that has a strong repulsive interaction with the ligands. A recent work of Shimoni-Livny et al.[22] has shown that hemidirected coordination is preferred for a number of ligands between 2 and 5. Nevertheless, when the number of ligands becomes too high, the ligand−ligand repulsion prevails over the ligand−

TABLE 2: Valence Angles (°) of the Deprotonated Caffeic Acid (H_2CA^-) and of Its 1:1 Complex $Pb(H_2CA)(H_2O)_n^+$ ($n = 0-4$)

	H_2CA^-	$Pb(H_2CA)^+$	$Pb(H_2CA)(H_2O)^+$	$Pb(H_2CA)(H_2O)_2^+$	$Pb(H_2CA)(H_2O)_3^+$	$Pb(H_2CA)(H_2O)_4^+$
$C_1C_2C_3$	122.0	121.4	121.4	121.4	121.4	121.4
$C_2C_3C_4$	116.8	118.6	118.6	118.5	118.4	118.4
$C_3C_4C_5$	121.2	120.1	120.2	120.2	120.3	120.3
$C_4C_5C_6$	121.2	120.4	120.4	120.5	120.5	120.5
$C_5C_6C_1$	118.6	120.0	119.8	119.7	119.7	119.6
$C_2C_3C_9$	120.1	118.1	118.3	118.4	118.4	118.4
$C_3C_9C_{10}$	128.2	128.0	128.3	128.4	128.5	128.5
$C_9C_{10}C_{11}$	123.3	120.8	120.9	121.2	120.9	121.6
$C_6C_1H_{14}$	118.6	118.6	118.6	118.6	118.6	118.6
$C_1C_2H_{15}$	119.4	119.6	119.5	119.4	119.4	119.4
$C_3C_4H_{16}$	119.4	120.5	120.4	120.5	120.4	120.4
$C_4C_5O_8$	123.8	126.3	125.9	125.7	125.6	125.6
$C_5O_8H_{17}$	108.3	111.8	111.4	111.3	111.2	111.2
$C_5C_6O_7$	120.4	120.1	120.2	120.2	120.2	120.3
$C_6O_7H_{18}$	106.2	109.3	109.0	108.8	108.7	108.7
$C_3C_9H_{19}$	116.8	115.9	115.6	115.5	115.5	115.3
$C_9C_{10}H_{20}$	121.8	123.4	123.3	123.3	123.2	122.9
$C_{10}C_{11}O_{12}$	115.9	123.9	123.6	123.1	123.3	122.4
$C_{10}C_{11}O_{13}$	113.7	121.7	121.1	120.7	120.2	120.6
$O_{12}C_{11}O_{13}$	130.4	114.4	115.3	116.2	116.5	116.9
$C_{11}O_{12}Pb$		91.8	92.2	92.0	92.4	96.1
$C_{11}O_{13}Pb$		92.0	91.8	92.2	93.2	90.3
$O_{12}PbO_{21}$			93.4	89.6	94.2	84.2
$O_{12}PbO_{22}$				72.4	75.6	79.4
$O_{12}PbO_{23}$					113.4	67.9
$O_{12}PbO_{24}$						90.8

lone pair one, and the arrangement evolves to holodirected. To estimate the coordination sphere of Pb(II) in the 1:1 complex $Pb(H_2CA)^+$, geometries of several complexes have been optimized, with a number of water molecules $n = 0-4$ (complexes $Pb(H_2CA)(H_2O)_n^+$). It can be seen in Figure 8 that all have hemidirected geometry.

Addition of water molecules on Pb(II) has only a minor effect on the parameters until $n = 3$. But it can be interesting to note that the general trend is to evolve toward the geometry of caffeate. All the bond lengths that increased between H_2CA^- and $Pb(H_2CA)^+$ decrease when the number of water molecules goes up, and vice versa. In $Pb(H_2CA)(H_2O)_3^+$, a differentiation between the two CO bonds of the carboxylate group is calculated. This is to rely to the nonequivalency observed for PbO_{12} and PbO_{13} bonds. The chelation to the carboxylate group becomes unsymmetrical. This observation is confirmed in $Pb(H_2CA)(H_2O)_4^+$, in which not only the gap between PbO_{12} and PbO_{13} is amplified, but also one water molecule is maintained in the lead environment only by an hydrogen bond formed with another water molecule. Indeed, the oxygen atom of a water molecule is 3.5 Å away from a lead ion, distance out of the bond length range (2.2−2.9 Å) generally observed, by X-ray diffraction, for such bonds in a solid-state complex.[24−26] This latter water molecule is located out of the coordination sphere of Pb(II), and it seems that a pentacoordination of Pb(II) constitutes a limit for this complex.

3.4. Vibrational Analysis. The low solubility of caffeic acid in water precludes the recording of infrared and Raman spectra of both caffeate and the 1:1 complex in solution. The record of infrared and Raman spectra of the 1:1 complex has been obtained on the solid compound. Under the experimental conditions defined in section 2.1, one is sure that only the complex of 1:1 stoichiometry is present in the solution, because the addition of lead was stopped before the complexation of the second site of the molecule.

Even if no experimental vibrational spectra could be obtained for caffeate, theoretical frequencies and vibrational normal mode assignment of this ion are reported in Table 3 (only the preponderant contributions are mentioned). Normal modes relative to the benzene ring have been labeled according to the convention used by Varsanyi for trisubstituted benzene,[27] adapted from the Wilson notation.[28] Vibrational mode assignments were made by visual inspection of vibrations animated by using the Molekel (version 4.3) program.[29] Due to the electronic delocalization provoked by the deprotonation of the carboxylic function, the $C_{11}{=}O_{12}$ stretching observed at 1687 cm^{-1} in the Raman spectrum of caffeic acid (and calculated at 1760 cm^{-1}) in methanol[11] is coupled with the $C_{11}O_{13}$ stretching in caffeate and gives rise to two calculated frequencies: 1688 and 1306 cm^{-1} that present a contribution of the asymmetric and symmetric C−O stretchings, respectively. Due to important couplings, the in-phase symmetric CO_2 stretch is calculated to be relatively low with respect to the usual carboxylate group. Except for some benzene ring normal modes, the theoretical spectrum exhibits numerous couplings between vibrators. The stretching vibrations relative to the aliphatic chain, and notably

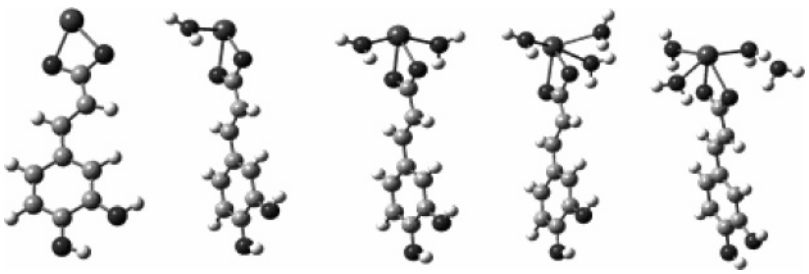

Figure 8. Calculated structure of $Pb(H_2CA)(H_2O)_n^+$ with $n = 0-4$.

TABLE 3: Calculated Frequencies (scaling factor 0.972) of the Mono-deprotonated Caffeic Acid (H_2CA^-) and Tentative Assignment According to Wilson's Notation for Benzene Ring (ν = stretching; δ = in-plane bending; γ = out-of-plane bending)

calculated	assignment
1688	$\nu_{as}(C_{11}O_{12}, C_{11}O_{13}) + \nu(C_9C_{10})$
1631	$8a + \nu(C_9C_{10})$
1622	$\nu(C_9C_{10}) + 8a$
1601	$8b + \nu(C_9C_{10})$
1519	19a
1441	19b
1371	$\delta(O_7H_{18})$
1316	$\nu(C_{10}C_{11}) + 14$
1306	$14 + \nu_s(C_{11}O_{12}, C_{11}O_{13}) + \nu(C_{10}C_{11})$
1284	$3 + \delta(C_9H_{19})$
1266	$\delta(C_9H_{19}, C_{10}H_{20}) + \nu(C_6O_7)$
1241	$3 + \delta(C_9H_{19}, C_{10}H_{20})$
1200	$\delta(O_7H_{18})$
1169	$\delta(O_7H_{18}, O_8H_{17}) + 18b$
1147	18a
1127	$18b + \nu(C_3C_9)$
1093	13
995	$\gamma(C_9H_{19}, C_{10}H_{20})$
954	$7b + \nu(C_3C_9)$
903	17b
890	$\delta_s(O_{12}C_{11}O_{13}) + \nu(C_{10}C_{11})$
865	$\gamma(C_9H_{19}, C_{10}H_{20})$
820	5
801	11
782	12
755	$1 + \delta(C_9C_{10}C_{11})$
706	$4 + \gamma(C_9H_{19}, C_{10}H_{20})$
689	$\delta_s(O_{12}C_{11}O_{13})$
656	$4 + \gamma(C_9H_{19}, C_{10}H_{20})$
591	16a
580	Δ_{mix}
540	6a
495	6b
444	Δ_{mix}
439	16b

for the C_3C_9 and $C_{10}C_{11}$ bonds, are distributed on a great number of normal modes, even if they do not always appear in the table. The two calculated frequencies at 580 and 444 cm^{-1} are assigned to rocking motions of the aliphatic chain mixed with a rocking of this chain with respect to the benzene ring (labeled Δ_{mix}).

The experimental frequencies of the infrared and Raman spectra, in the range 400−1800 cm^{-1}, of the 1:1 complex in the solid state are reported in Table 4. It is well-known that vibrational spectroscopy combined with theoretical frequency calculations is a powerful tool to determine the structural feature of chemical systems. So, to confirm the chelation of Pb(II) on the carboxylate group, vibrational frequencies of both $Pb(H_2CA)^+$ and $Pb(CA)^-$ (with lead ion coordinated to the carboxylate and catecholate group, respectively) have been calculated from their optimized geometries. Figure 9 allows the comparison, both in wavenumber and intensity, between the experimental Raman spectrum and calculated ones for $Pb(CA)^-$ and $Pb(H_2CA)^+$. It is obvious that the better agreement is found for the $Pb(H_2CA)^+$ form. From an intensity point of view, one can observe an inversion between the two theoretical profiles. For $Pb(CA)^-$ the high-intensity lines are located at low frequencies, whereas they are located in the 1100−1700 cm^{-1} spectral range for $Pb(H_2CA)^+$, in good accord with the experimental features. In the theoretical spectrum of $Pb(CA)^-$, only few frequencies are calculated in the high wavenumbers range, while the experimental spectrum and the calculated one for the other form show numerous lines in this same range. Indeed, all frequencies observed in the Raman and infrared spectra can easily be

TABLE 4: Experimental Vibrational Frequencies (Raman and infrared) of the 1:1 Stoichiometry Complex, Calculated Frequencies (scaling factor 0.972) of $Pb(H_2CA)(H_2O)_3^+$ Complex, and Tentative Assignment According to Wilson's Notation for Benzene Ring (ν = stretching; δ = in-plane bending; Δ = skeletal deformation; γ = out-of-plane bending)[a]

calculated	experimental		
$Pb(H_2CA)(H_2O)_3^+$	Raman	infrared	assignment
1620	1628		$8a + \nu(C_9C_{10})$
1592	1578		$\nu(C_9C_{10}) + 8a$
1584	1553		$8b + \nu(C_9C_{10})$
1525	1511	1522	$19a + \nu(C_9C_{10})$
1460	1485	1488	$19b + \nu(C_{11}O_{12}) + \nu(C_3C_9)$
1440			$\nu(C_{11}O_{12}) + \nu(C_{10}C_{11})$
1414	1412	1416	$\nu(C_{11}O_{13}) + \delta(O_7H_{18}) + \delta(C_{10}H_{20}) + \nu(C_{10}C_{11}) + 19b$
1385	1384	1389	$\delta(O_7H_{18}) + 19a + \nu(C_{11}O_{13})$
1342		1339	$\delta(O_7H_{18}, O_8H_{17}) + 14$
1313	1315		$\nu(C_9C_{10}) + \delta(C_9H_{19})$
1304	1300	1303	$\nu(C_6O_7) + 14$
1266	1261	1268	$3 + \delta(C_9H_{19,}C_{10}H_{20})$
1225	1242		$\delta(C_{10}H_{20})$
1184	1203	1208	$18a + \delta(O_7H_{18})$
1167	1166	1165	$\delta(O_7H_{18}, O_8H_{17}) + 18b$
1139			$18a + \delta(O_8H_{17})$
1108	1119	1117	$18a + \delta(O_8H_{17})$
994			$\gamma(C_9H_{19}) + \gamma(C_{10}H_{20})$
993			$\gamma(C_9H_{19}) + \gamma(C_{10}H_{20})$
964	977	977	7b
934			17b
857		856	$\gamma(C_{10}H_{20})$
832			11
810		811	5
805			$12 + \Delta$(chain)
773			$1 + \delta_s(O_{12}C_{11}O_{13})$
729			$\gamma(C_{10}C_{11}O)$
727	720	718	$\delta_s(O_{12}C_{11}O_{13}) + 12$
688			4
591		591	16a
584	584	579	Δ_{mix}
560			6a
518		517	$\gamma(O_7H_{18})$
507			$6b + \delta(C_3C_9C_{10})$
460		470	Δ_{mix}
438		419	16b
340			$\nu(PbO_{13})$
286			$\nu(PbO_{12})$

[a] Frequencies corresponding to water molecules vibrations are not reported. In low-frequency range (<400 cm^{-1}) only the Pb−O stretching frequencies are mentioned.

associated with theoretical ones calculated for $Pb(H_2CA)^+$. In opposition, some frequencies in the experimental spectrum have no counterpart in $Pb(CA)^-$ theoretical frequency set. For instance, in the ranges 1320−1530 cm^{-1} and 885−1130 cm^{-1}, four and two lines are, respectively, observed in the Raman spectrum and no frequency is calculated for $Pb(CA)^-$. One more time, this result validates the Pb(II) coordination on COO^-. So, vibrational frequencies have been calculated for $Pb(H_2CA)(H_2O)_n^+$ with $n = 0$, 1, 2, 3, and 4. Their theoretical spectra are rather close, one to each other. However, some frequency shifts can be observed according to the number of water molecules coordinated to lead ion. Indeed, mechanical couplings occurring in normal modes may slightly differ in the theoretical spectra of these compounds, but preponderant contributions remain identical. In all cases, a good agreement between theoretical and experimental spectra is obtained; however, the theoretical spectrum of $Pb(H_2CA)(H_2O)_3^+$ presents an agreement with the Raman and infrared spectra to some extent better than the others.

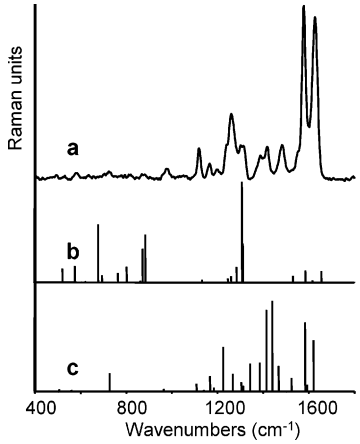

Figure 9. Experimental Raman spectrum of the complex 1:1 (a) and theoretical Raman spectra of the caffeic acid complex with Pb(II) coordinated to the catechol site (b) and the carboxylate site (c).

For this reason, only calculated wavenumbers of this last one are given in Table 4 with a tentative assignment.

Comparison of theoretical vibrational frequencies of free and complexed ligands (Tables 3 and 4) shows that the chelation of lead(II) induces more or less important changes in wavenumbers for almost all the normal modes. These spectral modifications are due to changes of mechanical couplings between the different vibrators, and one can notice that the number of couplings increases in the complex. Despite the fact that the chelation occurs on the carboxylate site, most of the quasi pure normal modes of the benzene ring are also very affected. They present frequency shifts from 0 (16a mode) to about 30 cm^{-1} (17b mode). This can be connected directly to the structural modifications of the ring previously observed for the complexed form. Both for free and complexed ligands, the C_9C_{10} stretching has a non negligible contribution in the four upper normal modes reported in the tables. The frequencies of these four modes considerably decrease in the complex; changes in the couplings and an increase of the C_9C_{10} bond length in $Pb(H_2CA)(H_2O)_3^+$ explain these shifts. In the opposite way, the C_3C_9 and $C_{10}C_{11}$ stretching modes are calculated at higher frequencies, in good accordance with the decrease of corresponding bond lengths in the complex. As observed in the structure of $Pb(H_2CA)(H_2O)_3^+$, the $C_{11}O_{12}$ and $C_{11}O_{13}$ bond lengths differ; consequently, no coupling is observed between the stretch of these bonds. However, the vibrations of these bonds are largely mixed with other vibrators.

If we consider, now, the comparison between experimental and calculated frequencies for the complex, one can notice that most of them are in good agreement. Some normal modes present a significant gap: calculated at 1584, 1460, and 1184 cm^{-1}, they are observed at 1553, 1485, and 1203 cm^{-1} in the Raman spectrum, respectively. But such discrepancies are not surprising, knowing that the comparison is made between frequencies calculated under a vacuum and measured on a sample in the solid state. Nevertheless, the average difference between experimental and calculated wavenumbers is relatively small: 8.5 cm^{-1}. The OH in plane bendings distributed on at least six normal modes are well calculated. They are observed at 1416 (1412), 1389 (1384), 1339, 1208 (1203), 1165 (1166), and 1117 (1119) cm^{-1} in the FTIR (Raman) spectra, and calculated at 1414, 1385, 1342, 1184, 1167, and 1108 cm^{-1}, respectively. This fact definitively confirms that the catechol function is not implicated in this complex. Three absorption bands (1488, 1416, and 1389 cm^{-1}) are observed in the infrared spectrum of the complex involving the ν(CO) of the carboxylate group. The frequencies of these bands are calculated at 1460, 1414, and 1385 cm^{-1} and could be assigned to $\nu(C_{11}O_{12})$, $\nu(C_{11}O_{13})$, and $\nu(C_{11}O_{13})$, respectively; these two stretchings are largely mixed with ring vibrations and with stretchings of the aliphatic chain. In the same manner, the Pb−O stretchings are not coupled because of the difference of bond lengths previously calculated. The $\nu(PbO_{13})$ and $\nu(PbO_{12})$ are, respectively, calculated at 340 and 286 cm^{-1}. These stretching modes are sensitive to the number of water molecules coordinated to the Pb ion (for instance, they were calculated at 374 and 352 cm^{-1} in $Pb(H_2CA)^+$). Unfortunately, no band is observed in the low wavenumber range of the Raman spectrum, that should have allowed the determination of the exact number of water molecules coordinated to Pb(II).

4. Conclusion

Complexation reactions of potentially toxic metals with naturally occurring organic molecules such as humic substances are being recognized as important factors in many natural systems, because these reactions determine the speciation and bioavailability of the metal species. The results of this study provide further information regarding the complexation of Pb(II) ions with caffeate, which can be considered as model molecule of humic substances. Both spectroscopic and theoretical approaches have allowed the comparison of catechol and carboxylate chelating power toward the lead ion. Among these two potential sites in competition within the molecular ion, we have demonstrated that the carboxylate group presents the greater complexing power toward Pb(II). The behavior of Pb(II) completely differs from that of Al(III), that preferentially coordinates the catechol group of the caffeic acid. The most predominant complexed form obtained for a small amount of lead nitrate is clearly the 1:1 complex, and the second chelating site is involved for $[Pb(II)]/[H_2CA^-]$ ratios higher than 0.3. The emission fluorescence spectra of the different species have been obtained by chemometric methods. Results of DFT calculations have shown that coordination of Pb(II) leads to important structural modifications of the ligand, and an electronic redistribution is observed in the complex. Structures and theoretical vibrational features of $Pb(H_2CA)(H_2O)_n^+$ with $n = 0-4$ have been investigated, all these species are bidentate and have a hemidirected distribution. Furthermore, we demonstrated that the coordination sphere is limited to 3 water molecules. A complete assignment of the vibrational spectra of both free and complexed ligands has been proposed from theoretical calculations. The Raman and infrared spectra of the 1:1 complex have permitted us to confirm the coordination of Pb^{2+} to the carboxylate group.

This study points out that no extrapolation can be made concerning the site preferentially implicated in the complexation mechanism of metal ion by caffeic acid, since the nature of the complex varies with the considered ion.

Acknowledgment. This work is part of the "Programme de Recherche Concertée: Sites et Sols Pollués" supported by the "Region Nord-Pas de Calais" and the "Fonds Européen de Développement Economique des Régions" (FEDER). "Institut du Développement et des Ressources en Informatique Scientifique" (IDRIS - Orsay, France) is thankfully acknowledged for the CPU time allocation. The authors also thank the Lille University Computational Center.

References and Notes

(1) Stevenson, F. J. *Humus Chemistry: Genesis, Composition, Reactions*; Wiley: New York, 1982.

(2) Stevenson, F. J.; Vance, G. F. *The environmental chemistry of aluminium*; Sposito, G., Ed.; CRC: Boca Raton, FL, 1989; p 145.
(3) Olsen, R. A.; Brown, J. C.; Bennett, J. H.; Blume, D. *J. Plant. Nutr.* **1982**, *5*, 433.
(4) Timberlake, C. F. *J. Chem. Soc.* **1959**, 2795.
(5) Bizri, Y.; Cromer, M.; Lamy, I.; Scharff, J. P. *Analusis* **1985**, *13*, 128.
(6) Yoe, J. H.; Jones, L. *Ind. Eng. Chem. Anal.* **1944**, *16*, 11.
(7) Frisch, M. J.; Trucks, G. W.; Schlegel, H. B.; Scuseria, G. E.; Robb, M. A.; Cheeseman, J. R.; Montgomery, J. A., Jr.; Vreven, T.; Kudin, K. N.; Burant, J. C.; Millam, J. M.; Iyengar, S. S.; Tomasi, J.; Barone, V.; Mennucci, B.; Cossi, M.; Scalmani, G.; Rega, N.; Petersson, G. A.; Nakatsuji, H.; Hada, M.; Ehara, M.; Toyota, K.; Fukuda, R.; Hasegawa, J.; Ishida, M.; Nakajima, T.; Honda, Y.; Kitao, O.; Nakai, H.; Klene, M.; Li, X.; Knox, J. E.; Hratchian, H. P.; Cross, J. B.; Adamo, C.; Jaramillo, J.; Gomperts, R.; Stratmann, R. E.; Yazyev, O.; Austin, A. J.; Cammi, R.; Pomelli, C.; Ochterski, J. W.; Ayala, P. Y.; Morokuma, K.; Voth, G. A.; Salvador, P.; Dannenberg, J. J.; Zakrzewski, V. G.; Dapprich, S.; Daniels, A. D.; Strain, M. C.; Farkas, O.; Malick, D. K.; Rabuck, A. D.; Raghavachari, K.; Foresman, J. B.; Ortiz, J. V.; Cui, Q.; Baboul, A. G.; Clifford, S.; Cioslowski, J.; Stefanov, B. B.; Liu, G.; Liashenko, A.; Piskorz, P.; Komaromi, I.; Martin, R. L.; Fox, D. J.; Keith, T.; Al-Laham, M. A.; Peng, C. Y.; Nanayakkara, A.; Challacombe, M.; Gill, P. M. W.; Johnson, B.; Chen, W.; Wong, M. W.; Gonzalez, C.; Pople, J. A. Gaussian 03, Revision B.04; Gaussian, Inc.: Pittsburgh, PA, 2003.
(8) Becke, A. D. *J. Chem. Phys.* **1993**, *98*, 5648.
(9) Lee, C.; Yang, W.; Parr, R. G. *Phys. Rev. B* **1988**, *37*, 785.
(10) Scott, A. P.; Radom, L. *J. Phys. Chem.* **1996**, *100*, 16513.
(11) Cornard, J. P.; Lapouge, C. *J. Phys. Chem. A* **2004**, *108*, 4470.
(12) Specfit Global Analysis System; Spectrum software Associates: Marlborough, MA, 1993.
(13) Gampp, H.; Maeder, M.; Meyer, C. J.; Zuberbühler, A. *Talanta* **1986**, *33*, 943.
(14) Friedman, M.; Jürgens, H. S. *J. Agric. Food Chem.* **2000**, *48*, 2101.
(15) Caudron, A.; Cornard, J. P.; Merlin, J. C. Unpublished results.
(16) Adams, M. L.; O'Sullivan B.; Downard, A. J.; Powell, K. J. *J. Chem. Eng. Data* **2002**, *47*, 289.
(17) Khvan, A. M.; Kristallovich, E. L. *Chem. Nat. Compd.* **2001**, *37*, 72.
(18) Davidson, R. S. *J. Photochem. Photobiol. B* **1996**, *33*, 3.
(19) Konya, K.; Scaiano, J. C. *J. Photochem. Photobiol A* **1996**, *100*, 119.
(20) Smith, G. J.; Haskell, T. G. *J. Photochem. Photobiol. B* **2000**, *55*, 103.
(21) Manceau, A.; Boisset, M. C.; Sarret, G.; Hazemann, J. L.; Mench, M.; Cambier, P.; Prost, R. *Environ. Sci. Technol.* **1996**, *30*, 1540.
(22) Shimoni-Livny, L.; Glusker, J. P.; Bock, C. W. *Inorg. Chem.* **1998**, *37*, 1853.
(23) Claudio, E. S.; ter Horst, M. A.; Forde, C. E.; Stern, C. L.; Zart, M. K.; Godwin, H. A. *Inorg. Chem.* **2000**, *39*, 1391.
(24) Esteban, D.; Avecilla, F.; Platas-Iglesias, C.; Mahia, J.; de Blas, A.; Rodriguez-Blas, T. *Inorg. Chem.* **2002**, *41*, 4337.
(25) Sanchiz, J.; Esparza, P.; Villagra, D.; Dominguez, S.; Mederos, A.; Brito, F.; Araujo, L.; Sanchez, A.; Arrieta, J. M. *Inorg. Chem.* **2002**, *41*, 6048.
(26) Thompson, L. K.; Zhao, L.; Xu, Z.; Miller, D. O.; Reiff, W. M. *Inorg. Chem.* **2003**, *42*, 128.
(27) Varsanyi, G. *Assignment for vibrational spectra of seven hundreds benzene derivatives*; Lang, L., Ed.; Hilger: Budapest, 1974.
(28) Wilson, E. B. *Phys. Rev.* **1934**, *45*, 706.
(29) Flükiger, P.; Lühti, H. P.; Portmann, S.; Weber, J. Molekel 4.3; Swiss Center for Scientific Computing: Manno (Switzerland), 2002.